Acta Crystallographica Section C
Crystal Structure Communications
ISSN 0108-2701

2-(Benzoylsulfanyl)acetic acid and 2,5-dioxopyrrolidin-1-yl 2-(benzoylsulfanyl)acetate by powder X-ray diffraction studies

Mwaffak Rukiah* and Mahmoud Al-Ktaifani

Department of Chemistry, Atomic Energy Commission of Syria (AECS), PO Box 6091, Damascus, Syrian Arab Republic
Correspondence e-mail: cscientific@aec.org.sy

Received 6 January 2011
Accepted 18 March 2011
Online 14 April 2011

The structures of the title compounds, $C_9H_8O_3S$, (I), and $C_{13}H_{11}NO_5S$, (II), were determined by X-ray powder diffraction. Both were solved using the direct-space parallel tempering algorithm and refined using the Rietveld method. In (I), the C—S—C bond angle is slightly smaller than normal, indicating more *p* character in the bonding orbitals of the S atom. The carboxylic acid group joins across an inversion centre to form a dimer. The crystal packing includes a weak C—H···O hydrogen bond between an aromatic C—H group and a carboxylic acid O atom to form a two-dimensional network parallel to $(10\bar{1})$. The C—S—C bond angle in (II) is larger than its counterpart in (I), indicating that the S atom of (II) has less *p* character in its bonding orbitals than that of (I), according to Bent's rule. The crystal structure of (II) includes weak C—H···O hydrogen bonds between the H atoms of the methylene groups and carbonyl O atoms, forming a three-dimensional network.

Comment

S-Benzoyl mercaptoacetic triglycine (S-Bz-MAG3) is widely used in radiopharmaceutical applications in nuclear medicine after labelling with ^{99m}Tc or ^{188}Re for kidney imaging (Guhlke *et al.*, 1998; Van Gog *et al.*, 1998; Hjelstuen *et al.*, 1998). As part of our interest in preparing S-Bz-MAG3 for pharmaceutical applications using literature methods (Brandau *et al.*, 1988; Schneider *et al.*, 1984; Xiuli *et al.*, 2003), and during the course of these preparations, the two title precursors of Bz-MAG3, *viz.* 2-(benzoylsulfanyl)acetic acid, (I), and 2,5-dioxopyrrolidin-1-yl 2-(benzoylsulfanyl)acetate, (II), were isolated. These compounds have a tendency to crystallize as very fine white powders. No crystal of sufficient thickness and quality could be obtained to perform a single-crystal analysis, hence laboratory powder X-ray diffraction was used to solve and refine their crystal structures. This involves a 13-atom (non-H) problem for (I) and a 20-atom (non-H) problem for (II). The crystal structures of a number of pharmaceutical compounds have been determined from X-ray powder data as a last resort in the absence of single crystals of sufficient quality (Chan *et al.*, 1999; Shankland *et al.*, 2001; Chernyshev *et al.*, 2003; Kiang *et al.*, 2003; Rukiah *et al.*, 2004; Van der Lee *et al.*, 2005; Rukiah & Assaad, 2010; Al-Ktaifani & Rukiah, 2010).

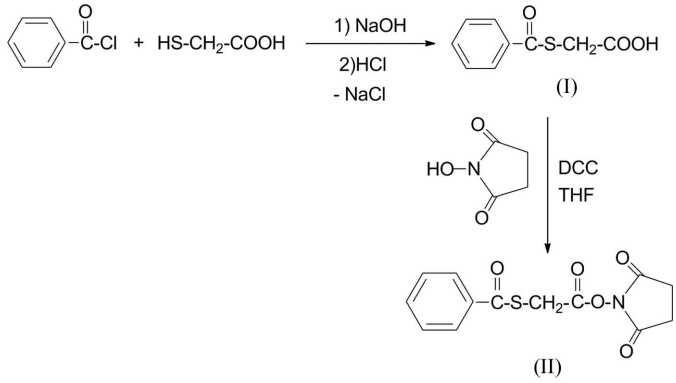

For success in a structure determination from powder diffraction data, the method is long and difficult before the final refinement step. This final step is commonly realised using the Rietveld method. Initial attempts to solve the structures of (I) and (II) by direct methods with the program *EXPO2004* (Altomare *et al.*, 2004) failed. The structures were solved with Monte Carlo simulated annealing (parallel tempering algorithm) from powder patterns in direct space using the program *FOX* (Favre-Nicolin & Černý, 2002). *FOX* solves structures by altering the positions, orientations and conformations of the molecule(s) in the unit cell according to the constraints of the space-group symmetry, until a good match is obtained between the calculated and observed intensities. One molecule was introduced randomly into the unit cell, which was calculated by Le Bail refinement. The H atoms can be ignored during the structure-solution process

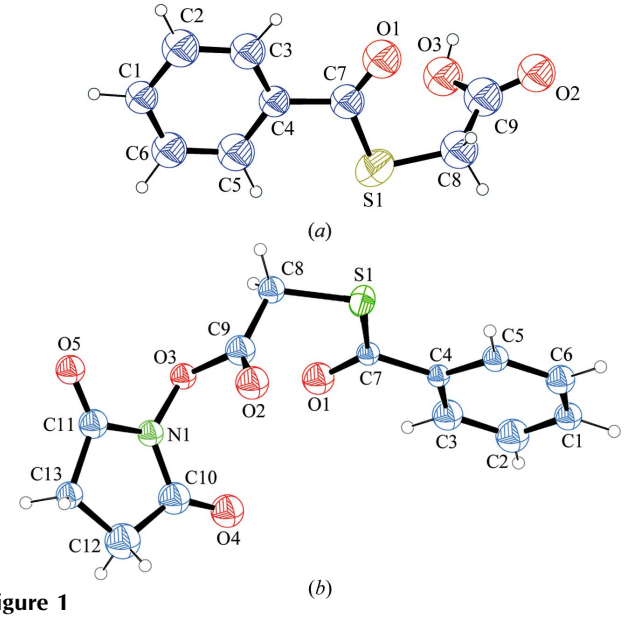

Figure 1
The molecular structures of (*a*) (I) and (*b*) (II). Displacement ellipsoids are drawn at the 30% probability level.

  doi:10.1107/S0108270111010328

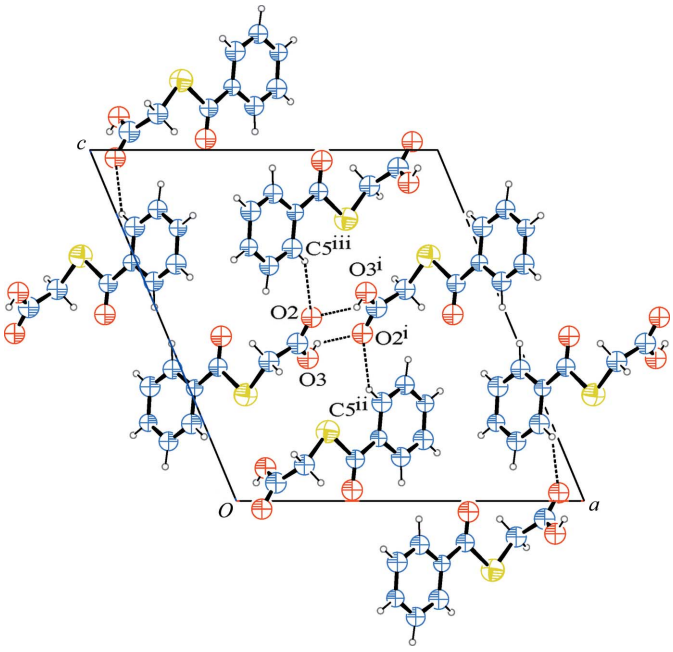

Figure 2
A view of the crystal structure of (I) along the *b* axis. Hydrogen bonds are indicated by dotted lines. [Symmetry codes: (i) $-x+1, -y+1, -z+1$; (ii) $-x+\frac{1}{2}, y+\frac{1}{2}, -z+\frac{1}{2}$; (iii) $x+\frac{1}{2}, -y+\frac{1}{2}, z+\frac{1}{2}$.]

because they do not contribute significantly to the powder diffraction pattern, due to their low X-ray scattering power. During the parallel tempering calculations, the molecule had the possibility of translating, rotating around its centre of mass and modifying its torsion angles. The molecule of (I) has four independent torsion angles and there are thus ten degrees of freedom for determination of the starting model by *FOX*. On the other hand, the molecule of (II) has six independent torsion angles, which indicates that there are 12 degrees of freedom for determining the starting model.

Compound (I) crystallizes with one molecule in the asymmetric unit in the space group $P2_1/n$ (Fig. 1*a*). In (I), atoms C7, S1 and O1 of the C_6H_5–CO–S fragment lie almost in the same plane, which is also that of the benzene ring. Atoms C8, C9, O2 and O3 of the C–COOH fragment are coplanar and roughly perpendicular to the plane of the C_6H_5–CO–S fragment and the C_6H_5 ring. The C—S—C bond angle [97.9 (3)°] is smaller than the normal value for tetrahedral geometry (109.5°). This observation indicates more *p* character in the bonding orbitals of the S atom in (I) (causing a reduced C—S—C bond angle), according to Bent's rule (Huheey *et al.*, 1993).

As shown in Fig. 2, the crystal structure of (I) is stabilized by hydrogen bonds (Table 1). The molecules are joined into hydrogen-bonded dimers across an inversion centre. These dimers are then joined by weak aromatic C—H···O hydrogen bonds to form a two-dimensional network parallel to $(10\bar{1})$.

Compound (II) crystallizes with one molecule in the asymmetric unit in the space group $P\bar{1}$ (Fig. 1*b*). Its structure is similar to that of (I), except that the H atom in the COOH group of (I) is replaced by a five-membered $N(COCH_2)_2$ ring in (II). This ring is effectively planar, with a maximum deviation of −0.044 (6) Å for atom C13 (average C—C bond

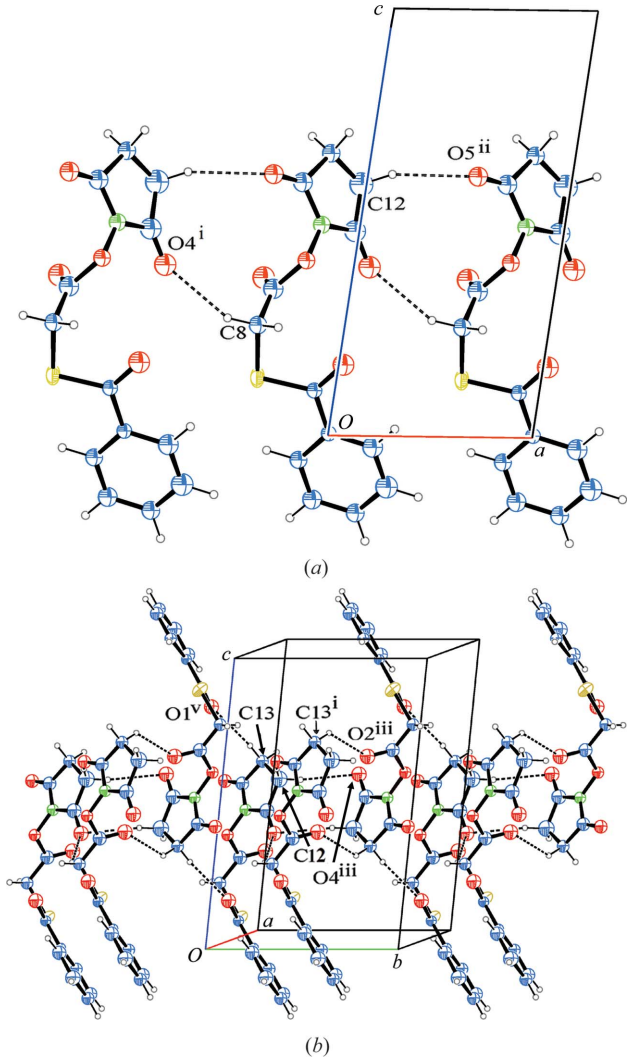

Figure 3
(*a*) Molecules of (II), linked into chains by weak C—H···O hydrogen-bonding contacts, viewed along the *b* axis. (*b*) Molecules of (II), linked into two-dinemsional networks by weak C—H···O hydrogen-bonding contacts, viewed along the *a* axis. Nonclassical hydrogen bonds are indicated by dotted lines. [Symmetry codes: (i) $x-1, y, z$; (ii) $x+1, y, z$; (iii) $-x, -y+1, -z+1$; (iv) $-x-1, -y+1, -z+1$; (v) $-x, -y, -z+1$.]

distance = 1.499 Å and C—C—C bond angle = 107.4°). A major point in the structure dimensions is that each pair of chemically equivalent N—C and C═O bonds in the five-membered ring has significantly different bond lengths (Table 2). Similar observations were reported for the parent molecule *N*-hydroxysuccinimide (Jones, 2003). This could be attributed to delocalization resulting from conjugation between the N-atom nonbonding pair [the tricoordinate N atom is planar and the sum of the angles around it is 359.9 (12)°] and one of the carbonyl groups (specifically, C10—O4), which increases the C═O bond length (reduces the double-bond character) and decreases the N—C bond lengths (increases the double-bond character). It is noteworthy that the C—S—C bond angle of 100.0 (3)° in (II) is larger than its counterpart in (I) [97.9 (3)°]; this gives an indication that the S atom of (II) has less *p* character in the bonding orbitals than that in (I), according to Bent's rule.

The crystal structure of (II) is stabilized by weak C—H···O hydrogen-bonding contacts (Table 3). Molecules related only by translation are linked into chains parallel to [100] by interactions between the central methylene (C8—H) and one pyrrolidine methylene (C12—H) group with pyrrolidine O atoms (Fig. 3*a*). Additional C—H···O interactions involving more methylene H atoms link molecules across centres of inversion, thereby completing two-dimensional networks which lie parallel to the (001) plane (Fig. 3*b*).

Experimental

Benzoyl chloride, mercaptoacetic acid, dicyclohexylcarbodiimide and *N*-hydroxysuccinimide were commercial samples and used as received. ^{1}H and ^{13}C{^{1}H} NMR spectra were recorded on a Bruker Bio Spin 400 spectrometer. IR spectra were recorded on an FT–IR Jasco 300E. Microanalysis was performed using a EURO EA instrument. X-ray powder diffraction patterns were obtained using a Stoe Stadi P diffractometer with monochromatic Cu $K\alpha_1$ radiation (λ = 1.5406 Å) selected with an incident-beam curved-crystal Ge(111) monochromator, using Stoe transmission geometry (horizontal set-up) with a linear position-sensitive detector (PSD).

For the preparation of (I), benzoyl chloride (14.05 g, 0.10 mol) was added dropwise to an aqueous solution of NaOH (0.22 mol) and mercaptoacetic acid (9.2 g, 0.12 mol) at 273 K and the mixture stirred at room temperature overnight. The organic layer was separated and washed with distilled water. The aqueous solutions were combined and acidified to pH 1.5 by adding concentrated HCl to obtain a white precipitate, which was separated and washed with ether to afford a white powder. Further purification of the product was achieved by recrystallization from ethyl acetate at 263 K (yield 11.8 g, 60%; m.p. 377 K). Analytical data for $C_9H_8O_3S$: found C 55.97, H 4.08, S 16.95%; required: C 55.09, H 4.11, S 16.34%. Spectroscopic analysis: IR (KBr, ν, cm^{-1}): 1710, 1670 (C═O), 3400 (OH), 1450 (aromatic C···C), 1200 (C—S—CO); ^{1}H NMR (400 MHz, $CDCl_3$, 298 K): δ 8.02 (*m*, aromatic, 2H), 7.63 (*m*, aromatic, 1H), 7.51 (*m*, aromatic, 2H), 3.95 (*s*, CH_2, 2H), 9.58 (*br*, COOH, 1H); ^{13}C{^{1}H} NMR (100 MHz, $CDCl_3$, 298 K): δ 31.1 (*s*, CH_2), 127.52 (*s*, aromatic), 128.81 (*s*, aromatic), 134.04 (*s*, aromatic), 135.90 (*s*, aromatic), 174.58 (*s*, CO), 190.12 (*s*, COOH).

For the preparation of (II), a solution of dicyclohexylcarbodiimide (DCC; 6.02 g, 0.03 mol) in tetrahydrofuran (THF, 20 ml) was added dropwise over a period of 20 min to a solution of (I) (4.8 g, 0.02 mol) and *N*-hydroxysuccinimide (2.80 g, 0.02 mol) in THF (60 ml) at 268 K. The mixture was stirred at this temperature for 2 h and after that at room temperature overnight. Glacial acetic acid (1 ml) was added to the mixture, which was then stirred for a further hour. A white precipitate (*N*,*N*′-dicyclohexylurea) was filtered off and washed twice with boiling THF. The filtrates were combined and evaporated to give a crude product. Purification of the product was achieved by recrystallization from ethyl acetate at 268 K to give a white powder (yield 3.3 g, 55%; m.p. 408 K). Analytical data for $C_{13}H_{11}O_5NS$: found C 54.20, H 4.15, S 11.70%; required: C 53.24, H 3.78, S 10.93%. Spectroscopic analysis: IR (KBr, ν, cm^{-1}): 1550–1850 (C═O), 1450 (aromatic C··· C), 1220 (C—S—CO); ^{1}H NMR (400 MHz, $CDCl_3$, 298 K): δ 8.01 (*m*, aromatic, 2H), 7.61 (*m*, aromatic, 1H), 7.51 (*m*, aromatic, 2H), 4.19 (*s*, CH_2, 2H), 2.83 (*s*, CH_2, 4H); ^{13}C{^{1}H} NMR (100 MHz, $CDCl_3$, 298 K): δ 25.58 (*s*, CH_2–ring), 28.28 (*s*, S—CH_2), 127.62 (*s*, aromatic), 128.87 (*s*, aromatic), 134.20 (*s*, aromatic), 135.59 (*s*, aromatic), 164.80 (*s*, COS), 168.65 (*s*, CO–ring), 188.66 (*s*, COO).

Table 1
Hydrogen-bond geometry (Å, °) for (I).

D—H···*A*	*D*—H	H···*A*	*D*···*A*	*D*—H···*A*
O3—H3O···O2^{i}	0.82	2.01	2.693 (8)	141
C5—H5···O2^{ii}	0.99	2.51	3.381 (7)	147

Symmetry codes: (i) $-x+1, -y+1, -z+1$; (ii) $x-\frac{1}{2}, -y+\frac{1}{2}, z-\frac{1}{2}$.

Compound (I)

Crystal data

$C_9H_8O_3S$
M_r = 196.22
Monoclinic, $P2_1/n$
a = 13.3928 (14) Å
b = 5.1432 (5) Å
c = 14.6577 (15) Å
β = 112.6458 (6)°
V = 931.81 (16) Å^3
Z = 4
Cu $K\alpha_1$ radiation, λ = 1.54060 Å
μ = 2.88 mm^{-1}
T = 298 K
Flat sheet, 7.0 × 7.0 mm

Data collection

Stoe Stadi P transmission diffractometer
Specimen mounting: powder loaded between two Mylar foils
Data collection mode: transmission
Scan method: step
Absorption correction: for a cylinder mounted on the φ axis (*GSAS*; Larson & Von Dreele, 2004)
T_{min} = 0.268, T_{max} = 0.303
$2\theta_{min}$ = 4.979°, $2\theta_{max}$ = 79.969°, $2\theta_{step}$ = 0.01°

Refinement

R_p = 0.022
R_{wp} = 0.028
R_{exp} = 0.026
$R(F^2)$ = 0.03399
χ^2 = 1.210
7500 data points
133 parameters
13 restraints
H-atom parameters constrained

Compound (II)

Crystal data

$C_{13}H_{11}NO_5S$
M_r = 293.30
Triclinic, $P\overline{1}$
a = 6.51605 (7) Å
b = 8.52612 (9) Å
c = 12.91910 (11) Å
α = 84.3274 (6)°
β = 80.5788 (6)°
γ = 69.1900 (4)°
V = 661.23 (1) Å^3
Z = 2
Cu $K\alpha_1$ radiation
λ = 1.5406 Å
μ = 2.37 mm^{-1}
T = 298 K
Flat sheet, 7.0 × 7.0 mm

Data collection

Stoe Stadi P transmission diffractometer
Specimen mounting: powder loaded between two Mylar foils
Data collection mode: transmission
Scan method: step
Absorption correction: for a cylinder mounted on the φ axis (*GSAS*; Larson & Von Dreele, 2004)
T_{min} = 0.327, T_{max} = 0.358
$2\theta_{min}$ = 4.975°, $2\theta_{max}$ = 79.965°, $2\theta_{step}$ = 0.01°

Refinement

R_p = 0.021
R_{wp} = 0.028
R_{exp} = 0.024
$R(F^2)$ = 0.01729
χ^2 = 1.440
7500 data points
228 parameters
21 restraints
H-atom parameters constrained

The powders of (I) or (II) were ground and loaded between two Mylar foils and fixed in a sample holder with a mask of suitable internal diameter (0.7 mm). Data were collected at room temperature

Table 2
Selected geometric parameters (Å, °) for (II).

S1—C7	1.740 (5)	C11—N1	1.396 (11)
S1—C8	1.796 (4)	C11—O5	1.184 (12)
C10—N1	1.377 (13)	N1—O3	1.403 (5)
C10—O4	1.200 (5)		
C7—S1—C8	100.0 (3)	C10—N1—O3	121.1 (7)
N1—C10—O4	124.3 (8)	C11—N1—O3	119.3 (7)
C10—N1—C11	119.5 (7)		

Table 3
Hydrogen-bond geometry (Å, °) for (II).

D—H···A	D—H	H···A	D···A	D—H···A
C8—H8B···O4^{i}	0.98	2.47	3.293 (9)	141
C12—H12A···O5^{ii}	0.98	2.55	3.488 (9)	159
C12—H12B···O4^{iii}	0.98	2.59	3.549 (9)	166
C13—H13A···O2^{iv}	0.98	2.57	3.307 (9)	132
C13—H13B···O1^{v}	0.98	2.50	3.458 (9)	166

Symmetry codes: (i) $x-1, y, z$; (ii) $x+1, y, z$; (iii) $-x, -y+1, -z+1$; (iv) $-x-1, -y+1, -z+1$; (v) $-x, -y, -z+1$.

and pressure over the angular range 5–80° (2θ), with a step length for the PSD of 0.5° (2θ) and with a counting time of 360 s per step for (I) and 420 s for (II).

Indexing was carried out using *DICVOL4.0* (Boultif & Louër, 2004), run with the default option. Confidence factors were $M(20)$ = 39.2 and $F(20)$ = 69.9 for (I), and $M(20)$ = 77.6 and $F(20)$ = 166.3 for (II). The most probable space group for (I) is $P2_1/n$, which was obtained using the program *CHECK-CELL* interfaced by *WINPLOTR* (Roisnel & Rodriguez-Carvajal, 2001), and the space group for (II) is $P\overline{1}$. In order to accelerate the process of structure solution with the program *FOX*, the powder pattern was truncated to 45° in 2θ (Cu $K\alpha_1$), corresponding to a real-space resolution of 2.0 Å. In the Rietveld refinement, carried out with the program *GSAS* (Larson & Von Dreele, 2004) interfaced by *EXPGUI* (Toby, 2001), the background was refined using a shifted Chebyshev polynomial with 23 coefficients. The Thompson–Cox–Hastings (Thompson *et al.*, 1987) pseudo-Voigt profile function was used with an axial divergence asymmetry correction (Finger *et al.*, 1994). The two asymmetry parameters of this function, S/L and D/L, were both fixed at 0.0225 during the Rietveld refinement. Geometric soft restraints were applied to the bond distances to guide them towards their normal values. Before the final refinement, the H atoms of the CH and CH_2 groups were introduced from geometric arguments. The hydroxy H atom was located in a difference Fourier map. The coordinates of the H atoms were refined as riding. The final refinement cycles were performed using unrestrained isotropic displacement parameters for C and O atoms and anisotropic displacement parameters for the S atom. For H atoms, a restrained isotropic refinement was used with $U_{iso}(H) = 1.2U_{eq}(C)$ or $1.5U_{eq}(O)$. No anomalous dispersion correction was applied. Intensities were corrected for absorption effects using a function for a flat-plate sample in transmission geometry with μd values which were determined experimentally for both compounds (μ is the absorption coefficient and d is the sample thickness). The preferred orientation was modelled using a spherical-harmonics description by Von Dreele (1997). The use of the preferred orientation correction leads to better molecular geometry with better agreement factors. The observed and calculated powder patterns for (I) and (II) are shown in Fig. 4.

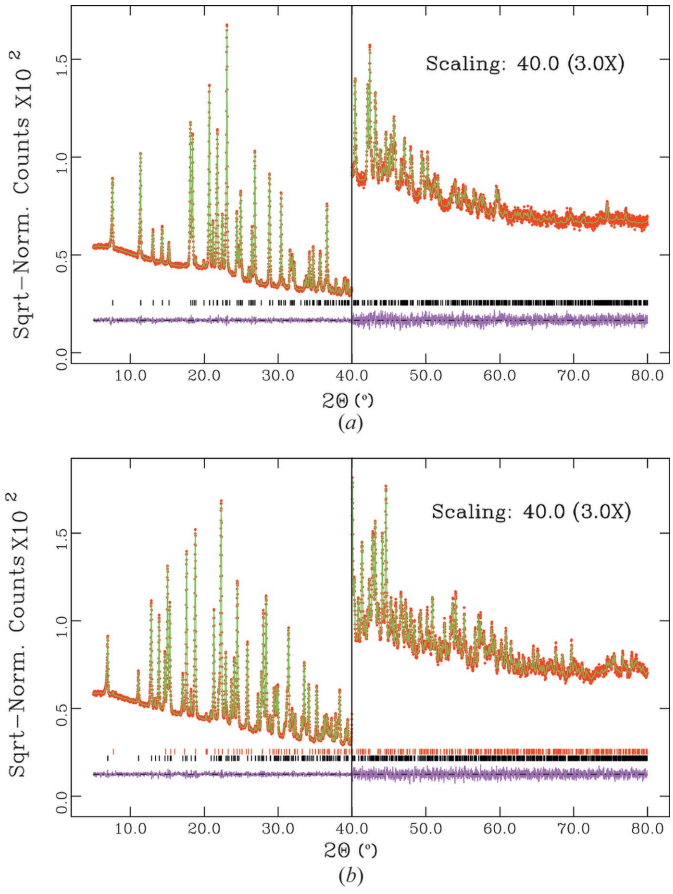

Figure 4
Final observed (points), calculated (line) and difference profiles for the Rietveld refinements of (*a*) (I) and (*b*) (II).

For both compounds, data collection: *WinXPOW* (Stoe & Cie, 1999); cell refinement: *GSAS* (Larson & Von Dreele, 2004); data reduction: *WinXPOW*; program(s) used to solve structure: *FOX* (Favre-Nicolin & Černý, 2002); program(s) used to refine structure: *GSAS*; molecular graphics: *ORTEP-3* (Farrugia, 1997); software used to prepare material for publication: *publCIF* (Westrip, 2010).

The authors thank Professor I. Othman, Director General, and Professor T. Yassine, Head of the Chemistry Department, for their support and encouragement of this work.

Supplementary data for this paper are available from the IUCr electronic archives (Reference: SK3399). Services for accessing these data are described at the back of the journal.

References

Al-Ktaifani, M. & Rukiah, M. (2010). *Acta Cryst.* C**66**, o479–o483.
Altomare, A., Caliandro, R., Camalli, M., Cuocci, C., Giacovazzo, C., Moliterni, A. G. G. & Rizzi, R. (2004). *J. Appl. Cryst.* **37**, 1025–1028.
Boultif, A. & Louër, D. (2004). *J. Appl. Cryst.* **37**, 724–731.
Brandau, W., Bubeck, B., Eisenhut, M. & Taylor, D. M. (1988). *Appl. Radiat. Isot.* **39**, 121–129.
Chan, F. C., Anwar, J., Cernik, R., Barnes, P. & Wilson, R. M. (1999). *J. Appl. Cryst.* **32**, 436–441.
Chernyshev, V. V., Machon, D., Fitch, A. N., Zaitsev, S. A., Yatsenko, A. V., Shmakov, A. N. & Weber, H.-P. (2003). *Acta Cryst.* B**59**, 787–793.

Farrugia, L. J. (1997). *J. Appl. Cryst.* **30**, 565.
Favre-Nicolin, V. & Černý, R. (2002). *J. Appl. Cryst.* **35**, 734–743.
Finger, L. W., Cox, D. E. & Jephcoat, A. P. (1994). *J. Appl. Cryst.* **27**, 892–900.
Guhlke, S., Schaffland, A., Zamora, P. O., Sartor, J., Diekmann, D., Bender, H., Knapp, F. F. & Biersack, H.-J. (1998). *Nucl. Med. Biol.* **25**, 621–631.
Hjelstuen, O. K., Tonnesen, H. H. & Bremer, P. O. (1998). *Nucl. Med. Biol.* **25**, 651–657.
Huheey, E. J., Keiter, E. A. & Keiter, R. L. (1993). *Inorganic Chemistry: Principles of Structure and Reactivity*, 4th ed. New York: HarperCollins College Publishers.
Jones, P. G. (2003). *Acta Cryst.* E**59**, o1951–o1952.
Kiang, Y. H., Huq, A., Stephens, P. W. & Xu, W. (2003). *J. Pharm. Sci.* **92**, 1844–1853.
Larson, A. C. & Von Dreele, R. B. (2004). *GSAS*. Report LAUR 86-748. Los Alamos National Laboratory, New Mexico, USA.
Roisnel, T. & Rodriguez-Carvajal, J. (2001). *Mater. Sci. Forum*, **378–381**, 118–123.
Rukiah, M. & Assaad, T. (2010). *Acta Cryst.* C**66**, o475–o478.
Rukiah, M., Lefebvre, J., Hernandez, O., van Beek, W. & Serpelloni, M. (2004). *J. Appl. Cryst.* **37**, 766–772.
Schneider, R. F., Subramanian, G., Feld, T. A., McAfee, C., Zapf-Longo, J. G., Palladino, E. & Thomas, F. D. (1984). *J. Nucl. Med.* **25**, 223–229.
Shankland, N., David, W. I. F., Shankland, K., Kennedy, A. R., Frampton, C. S. & Florence, A. J. (2001). *Chem. Commun.* pp. 2204–2205.
Stoe & Cie (1999). *WinXPOW*. Stoe & Cie, Darmstadt, Germany.
Thompson, P., Cox, D. E. & Hastings, J. B. (1987). *J. Appl. Cryst.* **20**, 79–83.
Toby, B. H. (2001). *J. Appl. Cryst.* **34**, 210–213.
Van der Lee, A., Richez, P. & Tapiero, C. (2005). *J. Mol. Struct.* **743**, 223–228.
Van Gog, F. B., Visser, G. W. M., Growising, R. W. A., Snow, F. B. & van Dongen, G. A. M. S. (1998). *Nucl. Med. Biol.* **25**, 611–619.
Von Dreele, R. B. (1997). *J. Appl. Cryst.* **30**, 517–525.
Westrip, S. P. (2010). *J. Appl. Cryst.* **43**, 920–925.
Xiuli, Z., Yongxian, W., Junling, L. & Duanzhi, Y. (2003). *J. Radioanal. Nucl. Chem.* **256**, 339–343.